

# FUSION OF SYNTHETIC APERTURE RADAR AND HYPERSPECTRAL IMAGERY TO DETECT IMPACTS OF OIL SPILL IN GULF OF MEXICO

*Lalitha Dabbiru<sup>1</sup>, Sathishkumar Samiappan<sup>1</sup>, Rodrigo A. A. Nobrega<sup>2</sup>, James A. Aanstoos<sup>1</sup>, Nicolas H. Younan<sup>3</sup>, and Robert J. Moorhead II<sup>1</sup>*

<sup>1</sup> Geosystems Research Institute, Mississippi State University, Mississippi State, MS 39762

<sup>2</sup> Institute of Geosciences, Federal University of Minas Gerais, Brazil

<sup>3</sup> Department of Electrical and Computer Engineering, Mississippi State University, Mississippi State, MS 39762

## ABSTRACT

The Deepwater Horizon blowout in the Gulf of Mexico resulted in one of the largest accidental oil disasters in U.S. history. NASA acquired radar and hyperspectral imagery and made them available to the scientific community for analyzing impacts of the oil spill. In this study, we use the L-band quad-polarized radar data acquired by Unmanned Aerial Vehicle Synthetic Aperture Radar (UAVSAR) and Hyperspectral Imagery (HSI) from the Airborne Visible/Infrared Imaging Spectrometer (AVIRIS) optical sensor. The main objective of this research is to apply fusion techniques on polarimetric radar and hyperspectral imagery to investigate the benefit of fusion for improved classification of coastal vegetation contaminated by oil. In this approach, fusion is implemented at the pixel level by concatenating the hyperspectral data with the high resolution SAR data and analyze the fused data with Support Vector Machine (SVM) classification algorithm.

**Index Terms**— PolSAR and hyperspectral data, Deepwater Horizon oil spill, data fusion, support vector machine

## 1. INTRODUCTION

The Deepwater Horizon blowout in the Gulf of Mexico occurred due to the rig exploded off the Louisiana coast on April 20, 2010. More than 200 million gallons of oil spewed into the Gulf of Mexico and the petroleum hydrocarbons were released from the reservoir through the wellbore for 87 days causing an oil spill of national significance. The oil spill caused significant damage to the environment and to the marine habitats. The damages associated with the oil spill include oiled and dead wildlife, polluted marshes, and lifeless deep water corals. In response to the Deepwater Horizon Oil Spill disaster in Gulf of Mexico, NASA acquired several synthetic aperture radar (SAR) and hyperspectral images (HSI) and made them available to the

scientific research community for analyzing impacts of the oil spill. SAR has been successfully used for detecting oil spills [1] [2]. Image fusion techniques are shown to be effective for detecting oils spills with SAR imagery [3]. Toxic compounds in petroleum hydrocarbons can cause severe stress to the vegetation along the shore line and this may result in changes of leaf color and could permanently damage the canopy. Spectral richness of HSI imagery enables the detection of subtle difference in vegetation stress [4][5]. Airborne HSI and other satellite imagery has been used in investigating Deepwater Horizon oil spill [6] [7].

## 2. STUDY AREA AND DATA USED

The coastal areas affected by Deepwater Horizon oil spill as of 19<sup>th</sup> June 2010 are shown in Figure 1. The areas outlined in red are heavily oiled; orange and green outlines indicate moderate and very light oiling respectively. The study area is near Wilkinson Bay, Louisiana, which was heavily impacted by oil. UAVSAR data collected on June 23, 2010 and AVIRIS data collected on July 31, 2010 were used in this study. Figure 1 shows the study area and a field photo of oiled and dead vegetation near Wilkinson Bay, Louisiana.

A high resolution aerial photograph of the study area is shown in Figure 2(a), a color composite of the UAVSAR 3-band (HH, HV, and VV) image is shown in Figure 2(b); and a false color composite of the AVIRIS image subset is shown in 2(c). The SAR and HSI images were co-registered and six ground truth classes were defined for investigation. The ground truth classes and the number of pixels in each class for SAR and HSI data are given in Table 1. These classes are: vegetation with heavy oiling, vegetation with very light oiling, water, water with oil, healthy vegetation and vegetation with moderate oiling.

The NASA AVIRIS is a 224 channel hyperspectral instrument with spectral coverage from 400 – 2500

nanometers (nm). The AVIRIS data collected on July 31, 2010 has a spatial resolution of 9.57 meters. The L-band UAVSAR data with HH (horizontal send and receive), HV (cross polarized), and VV (vertical send and receive) polarizations and a spatial resolution of 1.85 meters was used in this study. The size of SAR subset is 1316 x 402 pixels and the size of HSI subset is 284 x 83 pixels.

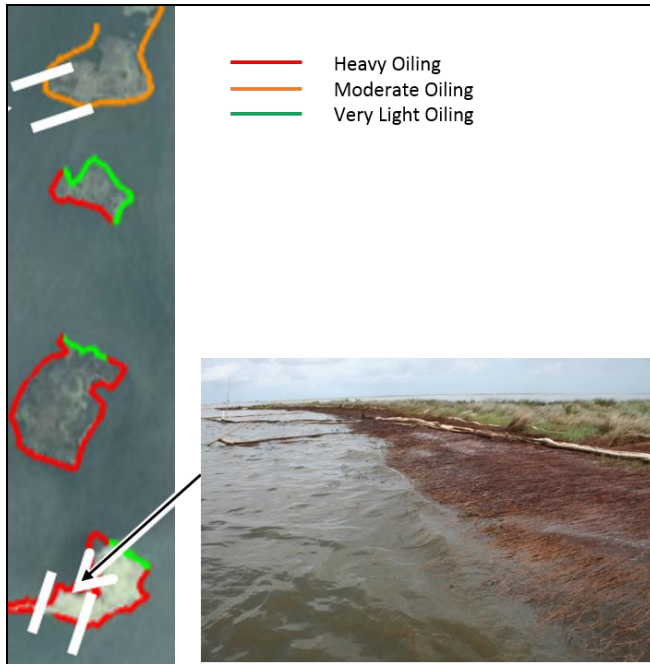


Figure 1: Coastal areas near Wilkinson Bay, Louisiana, affected by the Deepwater Horizon oil spill as of June 19, 2010 [8].

Table 1: Ground Truth Classes

Class Label	Name of class	Number of HSI Pixels	Number of SAR Pixels
C1	Vegetation with heavy oiling	32	398
C2	Vegetation with very light oiling	15	194
C3	Water	77	2161
C4	Water with oil	161	4119
C5	Healthy Vegetation	20	452
C6	Vegetation with moderate oiling	13	97

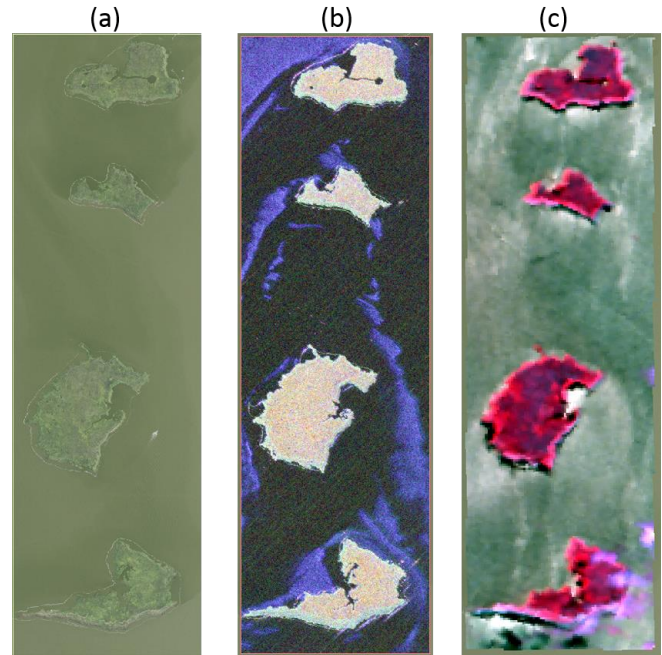


Figure 2: (a) Optical image of the study area, (b) Color composite of UAVSAR 3-band (HH, HV, and VV) image subset, and (c) Color composite of AVIRIS image subset.

### 3. DATA FUSION AND CLASSIFICATION

Data fusion may be performed at various information levels, such as pixel, feature, and decision level. Hsu *et al.* implemented fusion of hyperspectral and SAR imagery at both data and feature levels, resulting in a combined spatial-spectral analysis to enhance target identification [9]. Pixel level fusion was investigated on SAR and HSI data for detection of surface and buried mines, which resulted less false alarm rate [10]. In this study, fusion is implemented at the pixel level and Figure 3 shows the block diagram of the approach. The simulated SAR data were generated by taking the median of a 5 x 5 spatial window and concatenated with the HSI data.

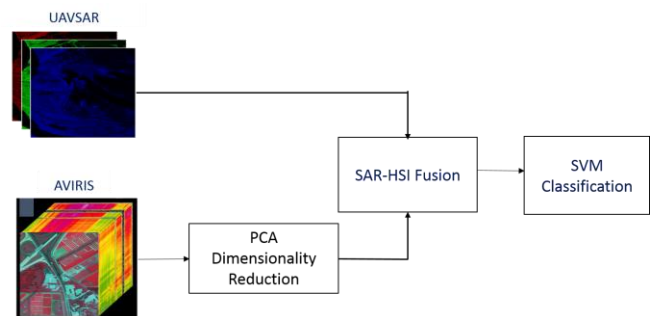


Figure 3: Block diagram of pixel level fusion of SAR and hyperspectral imagery

The support vector machine (SVM) is a powerful supervised learning method for analyzing and recognizing the patterns [11]. This research implemented the SVM classifier on the fused HSI-SAR dataset and on the extracted feature sets of individual sensors. 30% of labeled samples were used to train the classifier and the rest of the pixels were predicted by the classifier.

## 4. FEATURE EXTRACTION

### 4.1 HSI Features

In hyperspectral data, image information is concentrated in the principal components associated with large eigenvalues. Therefore, we applied principal component analysis (PCA) to achieve dimensionality reduction. Since there are six ground truth classes, the first five principal components were selected for analysis.

### 4.2 SAR Features

Grey Level Co-Occurrence Matrix (GLCM) features [12] were extracted from the SAR data in four spatial orientations: horizontal, left diagonal, vertical, and right diagonal corresponding to 0°, 45°, 90°, and 135°, and six features have been computed on each matrix with a window size of 11. The features used in this study are: energy, correlation, variance, homogeneity, entropy, and inertia.

## 5. RESULTS AND DISCUSSION

The classifier was tested with the following combinations of the features as shown in Table 2. The accuracy results for each of these combinations is shown in Figure 4. Overall, the HSI-SAR fusion performed as well as or better than the other combinations. The SAR-based features performed better on two classes: healthy vegetation (C5) and lightly oiled vegetation (C2). For all the other classes, the HSI-based features outperformed.

Table 2. Feature Combinations

SAR	HH, HV, and VV backscatter magnitudes (3 features)
SAR – GLCM	SAR with 36 GLCM features
HSI	224 HSI channels
HSI – PCA	5 HSI principal components
HSI – SAR Fusion	3 SAR bands (HH, HV, and VV) with 5 HSI principal components

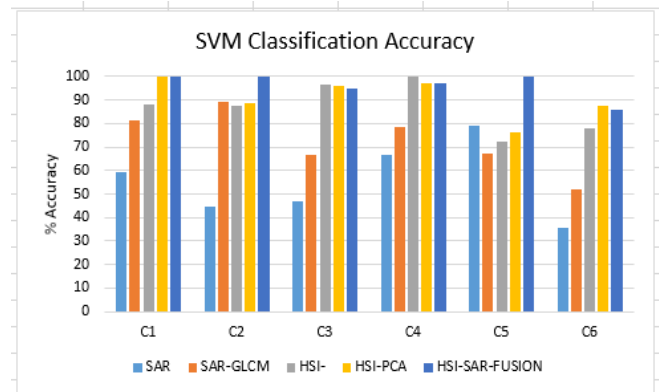


Figure 4: Classification accuracy (%) of SVM classifier with SAR polarization data (HH, HV, and VV bands), SAR with GLCM features, HSI without dimensionality reduction, HSI with PCA, and HSI-SAR fused data.

## 6. CONCLUSION

In this paper, fusion of SAR and HSI data was implemented at the pixel level for classification of areas affected by the oil spill in the Gulf of Mexico. Five different combinations of features derived from the HSI and SAR data were tested with SVM classifier. The results demonstrated the benefit of multi-sensor fusion with overall accuracy of the fused feature set exceeding that of either HSI or SAR alone.

## 7. ACKNOWLEDGEMENT

The authors would like to acknowledge NASA for providing the UAVSAR and AVIRIS data.

## 8. REFERENCES

- [1] F. Del Frate, D. Latini, A. Taravat, and C. E. Jones, "A novel multi-band SAR data technique for fully automatic oil spill detection in the ocean," *Proc. SPIE*, vol. 8891, pp. 889105–889106, 2013.
- [2] B. Minchew, C. E. Jones, and B. Holt, "Polarimetric Analysis of Backscatter From the Deepwater Horizon Oil Spill Using L-Band Synthetic Aperture Radar," *IEEE Transactions on Geoscience and Remote Sensing*, vol. 50, no. 10, pp. 3812–3830, 2012.
- [3] L. Lopez, M. Moctezuma, and F. Parmiggiani, "Contextual approach for oil spill detection in SAR images using image fusion and markov random fields," *49th IEEE International Midwest Symposium on Circuits and Systems, 2006. MWSCAS '06*, vol. 2, pp. 137–139, 2006.

- [4] S. Samiappan, S. Prasad, L. M. Bruce, and W. Robles, "NASA's upcoming HyspIRI mission - precision vegetation mapping with limited ground truth," *IEEE Int. Geosci. Remote Sens. Symp. IGARSS 2010*.
- [5] S. Prasad, L. M. Bruce, and H. Kalluri, "A Robust Multi-Classifer Decision Fusion Framework for Hyperspectral, Multi-Temporal Classification," *IEEE International Geoscience and Remote Sensing Symposium*, 2008, vol. 2, pp. II-273-II-276.
- [6] I. Leifer, W. J. Lehr, D. Simecek-Beatty, E. Bradley, R. Clark, P. Dennison, Y. Hu, S. Matheson, C. E. Jones, B. Holt, M. Reif, D. A. Roberts, J. Svejksky, G. Swayze, and J. Wozencraft, "State of the art satellite and airborne marine oil spill remote sensing: Application to the BP Deepwater Horizon oil spill," *Remote Sens. Environ.*, vol. 124, pp. 185-209, Sep. 2012.
- [7] S. Khanna, M. J. Santos, S. L. Ustin, A. Koltunov, R. F. Kokaly, and D. A. Roberts, "Detection of Salt Marsh Vegetation Stress and Recovery after the Deepwater Horizon Oil Spill in Barataria Bay, Gulf of Mexico Using AVIRIS Data," *PLoS One*, vol. 8, no. 11, p. e78989, 2013.
- [8] K. Davis, A. Bruce, Kuper, Philip, Holecamp, "UAVSAR Validation-shoreline impact assesment."
- [9] Su May Hsu and Hsiao-Hua K. Burke, "Multisensor fusion with hyperspectral imaging data: Detection and classification," *Lincoln Laboratory Journal*, vol. 14, no.1, 2003.
- [10] Nasser M. Nasrabadi, "A nonlinear kernel-based joint fusion/detection of anomalies using hyperspectral and SAR imagery," *Proceedings of the IEEE International Conference on Image Processing (ICIP' 08)*, pp. 1864 - 1867, 2008.
- [11] V. Vapnik. Statistical Learning Theory. John Wiley and Sons, Inc., New York, 1998.
- [12] R. M. Haralick, K. Shanmugan, and I. H. Dinstein, "Textural features for image classification," *IEEE Trans. Syst., Man, Cybern.*, vol. SMC-3, pp. 610-621, May 1973.